

Measuring Visual Complexity of Cluster-Based Visualizations

B. Duffy¹, A. Dasgupta², R. Kosara², S. Walton¹, and M. Chen¹

¹ University of Oxford, UK

² University of North Carolina, Charlotte, USA

Abstract

Handling visual complexity is a challenging problem in visualization owing to the subjectiveness of its definition and the difficulty in devising generalizable quantitative metrics. In this paper we address this challenge by measuring the visual complexity of two common forms of cluster-based visualizations: scatter plots and parallel coordinatess. We conceptualize visual complexity as a form of visual uncertainty, which is a measure of the degree of difficulty for humans to interpret a visual representation correctly. We propose an algorithm for estimating visual complexity for the aforementioned visualizations using Allen's interval algebra. We first establish a set of primitive 2-cluster cases in scatter plots and another set for parallel coordinatess based on symmetric isomorphism. We confirm that both are the minimal sets and verify the correctness of their members computationally. We score the uncertainty of each primitive case based on its topological properties, including the existence of overlapping regions, splitting regions and meeting points or edges. We compare a few optional scoring schemes against a set of subjective scores by humans, and identify the one that is the most consistent with the subjective scores. Finally, we extend the 2-cluster measure to k-cluster measure as a general purpose estimator of visual complexity for these two forms of cluster-based visualization.

1. Introduction

Visual complexity is a pervasive problem in different domains such as graphical user interfaces, web information, visualizations, etc. While the correlation between visual complexity and cognitive load [HMS09] has been established, it is widely acknowledged that one of the main challenges is to provide an objective definition such that it bridges system-level behavior with user perception [SBSC10]. The subjectiveness of this notion makes it difficult to develop reliable metrics for measuring visual complexity.

The focus of this paper is to measure *visual complexity* in cluster visualization. We examine two forms of such visualization, namely scatter plots and parallel coordinatess [ID90]. Here we define visual complexity as a form of *visual uncertainty* [DCK12]. It measures visual components, such as overlapped points, lines and shapes, missing objects, and split or disconnected shapes, that may lead to confusion in viewing the visualization. Our contributions are:

- We propose a novel application of Allen's interval algebra for formulating a metric for measuring visual complexity.
- We show that the 13×13 topological cases in 2D can be reduced to 24 primitive cases for scatter plots and 35 primitive cases for parallel coordinates.

- We define two metrics for estimating visual complexity in scatter plots and parallel coordinates respectively and we make use of look-up tables in a manner similar to the marching cubes algorithm [LC87].
- We compare the scores of the two metrics with a set of subjective scores by humans, and confirm the two metrics are effective.

2. Related Work

In this section we discuss the relevant literature on clustered parallel coordinates and scatter plots, and on concepts of and metrics for visual complexity.

2.1. Clustered Scatter Plots and Parallel Coordinates

Traditional clustering techniques in visualization are of two main types: analytical clustering and visual clustering. Analytical clustering aims to maximize within cluster information by using data-space properties [FWR99, NH06]. Two-dimensional clusters that tend to overlap between axes [AA04] add to the visual complexity, but computational approaches to quantify that has been absent in the literature. Visual clustering in parallel coordinates aims to reduce clutter;

some examples include geometrically deforming and grouping poly-lines to overcome edge clutter [ZYQ*08] and use of high-precision textures for reducing the effect of overplotting [JLJC05]. Privacy-preserving clustering [DK11] encompasses these two categories, the goal here being controlling the within-cluster information to prevent disclosure. Quantifying complexity in terms of uncertainty measures have been found to be useful in quantifying the utility of privacy-preserving visualizations [withheld].

2.2. Visual Complexity Measures

Rosenholtz et al. [RLN07] describe a number of methods for measuring visual clutter and complexity based on the ideas of feature congestion and reaction time. They highlight the current state of the art for measuring visual complexity falls into two categories. Simplistic measures of visual complexity based on counting geometric primitives such as lines and triangles, and complex measures based on computer vision techniques. However, these methods have a number of drawbacks. The simplistic methods are generally used for visualization displays in two and three dimensions, making them dependant on the input data. In addition there is only a weak correlation between the number of primitives in the display and the complexity of the visual output [CDD06, SSD*08, KW10, DCT12]. The complex methods are computationally intense and not appropriate for visualization displays when access to raw geometric data is available. In general there is a lack of tools for measuring visual complexity in visualization applications that quantifies overlap and occlusion. Simplistic methods such as, counting geometric primitives, i.e., vertices, lines etc. have been used in visualization applications. This method has been applied recently by Carr et al. [CDD06], Scheidegger et al. [SSD*08] and Duffy et al. [DCT12] for measuring the complexity of isosurfaces through triangle counts and cell intersections. Khoury et al. [KW10] use fractal box dimensions to measure isosurface complexity. More complex computer vision methods are the alternative as illustrated by Rosenholtz et al. [RLN07].

2.3. Related Approaches: Clutter and Visual Quality

Clutter reduction techniques are important in the context of information visualization as they visual quality preserving rendering. Ellis and Dix have outlined in their taxonomy [ED07] how the different clutter reduction approaches fit in a common framework. There is a lack of agreeable definition of clutter [ED06] and visual quality [BS06]. While there have been approaches to define clutter in terms of outliers [PWR04], other researcher have defined clutter in terms of overlapping visual objects [AdOL04, DK10]. Similarly with visual quality, while quality metrics have been proposed to improve the perceptual aspect of visualizations, similar metrics have been suggested for pattern identification. We believe a decomposition of visualization in terms

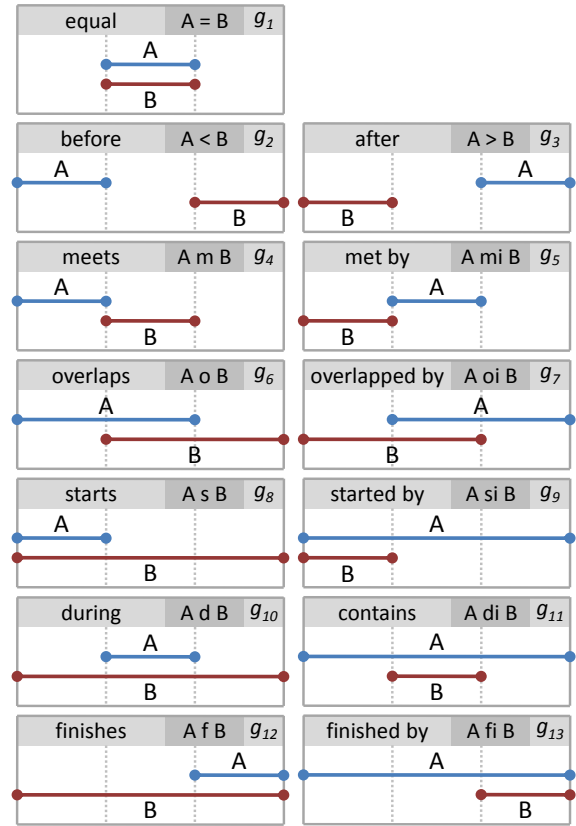


Figure 1: Allen algebra intervals in 1D. Shown are the 13 operators in the algebra.

of its smallest components, that is, the visual structures will enable us to standardize metrics across different visual representations. Moreover, quantification of complexity will also enable more concrete optimization processes that can minimize clutter on screen.

3. Allen's Interval Algebra

Allen developed an interval algebra in 1983 for reasoning about discrete time intervals [All83]. As shown Figure 1, the algebra defines a set of 13 operators on two interval operands in 1D. It is not difficult to observe that the operators exhibit some symmetry in relation to the ordering of the two operands. For the convenience mathematical representation, let us write each operation in a functional form akin to the Polish prefix notation:

$$g_i(A, B), \quad i = 1, 2, \dots, 13$$

where g_i is an operator (i.e., g_1 is $<$, g_2 is $>$, etc.), and A and B are the two interval operands, $[a_1, a_2]$ and $[b_1, b_2]$, such that $a_1 < a_2$ and $b_1 < b_2$. Note that the function g_i can be regarded as a Boolean function that determines whether

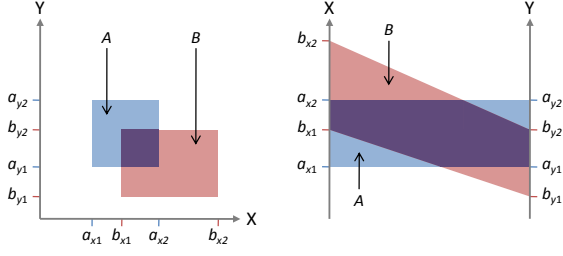


Figure 2: Simple case of overlapping clusters in scatter plots and parallel coordinates.

Allen's i^{th} relationship between A and B is true or false. The *Operand Ordering Symmetry* can thus be expressed as:

$$\Psi_{OOS}(g_i(A, B)) \rightarrow g_j(B, A), \quad 1 \leq i, j, \leq 13 \quad (1)$$

where Ψ_{OOS} is the *transformation* of swapping the two operands for a given $g_i(A, B)$. A symmetric relation holds if g_j exists. There are seven pairs of such symmetry, including the self-symmetry $g_1(A, B) = g_1(B, A)$.

Another form of symmetry results from flipping an axis towards the opposite direction. In 1D case, given an interval $X = [x_1, x_2]$, we denote its mirror on the flipped axis as $X^- = [-x_2, -x_1]$. Hence, the *Axis Flipping Symmetry* can be expressed as:

$$\Psi_{AFS}(g_i(A, B)) \rightarrow g_j(A^-, B^-), \quad 1 \leq i, j, \leq 13 \quad (2)$$

where Ψ_{AFS} is the transformation of flipping the axis. There are seven pairs of such symmetry, including $g_8(A, B) = g_{12}(A^-, B^-)$ and $g_9(A, B) = g_{13}(A^-, B^-)$.

With these two types of symmetry, we can reduce the 13 cases to 6 primitive cases, which are $g_1, g_2, g_4, g_8, g_{10}$ (=, <, m, o, s, d). Each of the other 7 cases can be inferred from a primitive case using one of the two symmetry relations.

4. 2-Cluster Overlaps

Allen's interval algebra can be extended to 2D when examining cases in two common forms of cluster visualization; namely scatter plots and parallel coordinates. In previous work Dasgupta and Kosara [DK10] used Allen's algebra for computing metrics for parallel coordinates. Figure 2 shows a simple case of two overlapping clusters in a scatter plot as well as a parallel coordinates. The relationship on the x -axis is AoB or $g_5(A, B)$, and that on the y -axis is $AoiB$ or $g_6(A, B)$. We can represent this case by the following 2-tuple:

$$[g_5(A, B), g_6(A, B)]$$

It is not difficult to observe that given an ordered pair of operands, there are $13 \times 13 = 169$ different tuples in 2D.

4.1. Symmetries in 2D and Primitive Cases

Using symmetry relationships, we have found that the 169 cases can be reduced to 24 primitive cases in scatter plots, and 35 primitive cases in parallel coordinates. The symmetry relationships shared by both types of plots are:

2D Operand Ordering Symmetry — This is a direct extrapolation from the same type of symmetry in 1D. Let A and B be two clusters, their ranges on the x -axis are A_x and B_x , and those on the y -axis are A_y and B_y respectively. We can express this symmetry in 2D using a transformation Ψ_{2d-OOS} as:

$$\begin{aligned} & \Psi_{2d-OOS}([g_i(A_x, B_x), g_s(A_y, B_y)]) \\ & \rightarrow [\Psi_{OOS}(g_i(A_x, B_x)), \Psi_{OOS}(g_s(A_y, B_y))] \quad (3) \\ & \rightarrow [g_j(B_x, A_x), g_t(B_y, A_y)] \end{aligned}$$

where $1 \leq i, j, s, t \leq 13$, and Ψ_{OOS} is the corresponding 1D transformation as B before and after the symmetric transformation, and similarly g_s and g_t for the y -axis.

Synchronized Axes Flipping Symmetry — We can also extrapolate the *Axis Flipping Symmetry* to 2D by flipping both axes simultaneously towards the opposite direction. We can express this symmetry as:

$$\begin{aligned} & \Psi_{SAFS}([g_i(A_x, B_x), g_s(A_y, B_y)]) \\ & \rightarrow [\Psi_{AFS}(g_i(A_x, B_x)), \Psi_{AFS}(g_s(A_y, B_y))] \quad (4) \\ & \rightarrow [g_j(A_x^-, B_x^-), g_t(A_y^-, B_y^-)] \end{aligned}$$

where $i, j, s, t, g_i, g_j, g_s, g_t$ are defined as previously with Ψ_{2d-OOS} .

Axes Ordering Symmetry — This is a new form of symmetry in 2D, which encodes the symmetric transformation, with which the orders of the two axes, X and Y are swapped in the visualization.

$$\Psi_{AOS}([g_i(A_x, B_x), g_s(A_y, B_y)]) \rightarrow [g_j(A_y, B_y), g_t(A_x, B_x)] \quad (5)$$

where $i, j, s, t, g_i, g_j, g_s, g_t$ are defined as previously, except that g_j now applies to the intervals on the y -axis, while g_t on the x -axis.

In addition, there is another type of symmetry that is more meaningful to scatter plots than to parallel coordinates plots. With scatter plots, if one flips either of the two axes individually, it does not change the topology or amount of overlapping between the two clusters, and thereby has limited impact on the perception of the visual complexity. On the contrary, flipping only one axis may cause a change of overlapping relationship in a parallel coordinates. Given two non-overlapping clusters, they would become overlapped after one of the two axes is flipped. Hence the following symmetry applies only to scatter plots.

Asynchronized Axis Flipping Symmetry — We use Ψ_{AxFS} to denote the transformation of flipping the x -axis, and Ψ_{AyFS} for that of the y -axis. Similar to Ψ_{SAFS} , these two

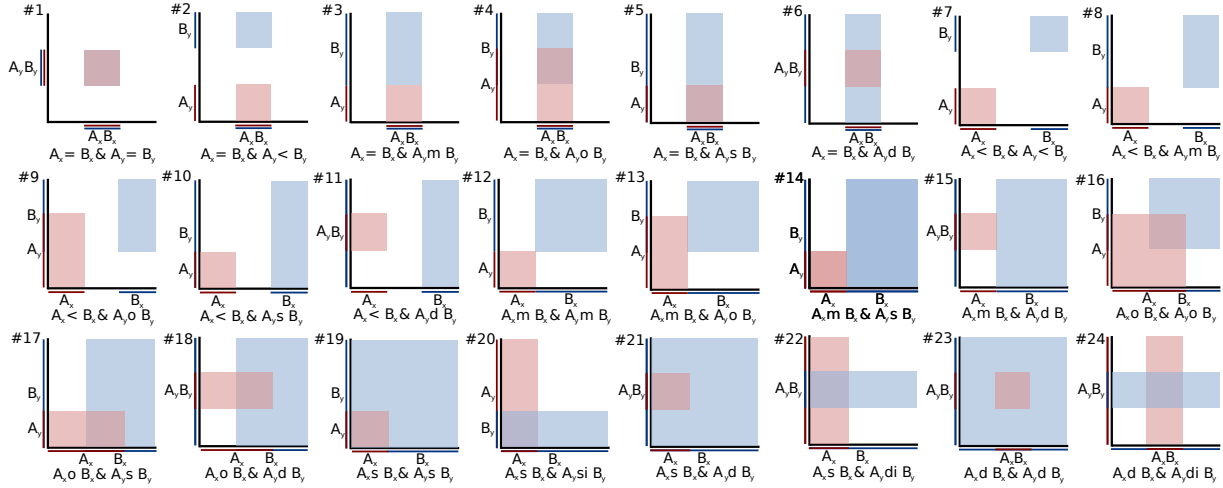


Figure 3: 169 scatter plot cases can be reduced to a subset of 24 topologically distinct bases cases using 4 symmetries.

y		g_1	g_2	g_3	g_4	g_5	g_6	g_7	g_8	g_9	g_{10}	g_{11}	g_{12}	g_{13}
		A = B	A < B	A > B	A m B	A mi B	A o B	A oi B	A s B	A si B	A d B	A di B	A f B	A fi B
g_1	A = B	#1	#2	→[1,2]	#3	→[1,4]	#4	→[1,6]	#5	→[1,8]	#6	→[1,10]	→[1,8]	→[1,12]
g_2	A < B	→[1,2]	#7	→[2,2]	#8	→[2,4]	#9	→[2,6]	#10	→[2,8]	#11	→[3,10]	→[3,9]	→[3,8]
g_3	A > B	→[1,3]	→[2,3]	→[2,2]	→[2,5]	→[2,4]	→[2,7]	→[2,6]	→[2,9]	→[2,8]	→[2,10]	→[2,10]	→[2,13]	→[2,12]
g_4	A m B	→[1,4]	→[2,4]	→[3,4]	#12	→[4,4]	#13	→[4,6]	#14	→[4,8]	#15	→[5,10]	→[5,9]	→[5,8]
g_5	A mi B	→[1,5]	→[2,5]	→[3,5]	→[4,5]	→[4,4]	→[4,7]	→[4,6]	→[4,9]	→[4,8]	→[4,10]	→[4,10]	→[4,13]	→[4,12]
g_6	A o B	→[1,6]	→[2,6]	→[3,6]	→[4,6]	→[5,6]	#16	→[6,6]	#17	→[6,8]	#18	→[7,10]	→[7,9]	→[7,8]
g_7	A oi B	→[1,7]	→[2,7]	→[3,7]	→[4,7]	→[5,7]	→[6,7]	→[6,6]	→[6,9]	→[6,8]	→[6,10]	→[6,10]	→[6,13]	→[6,12]
g_8	A s B	→[1,8]	→[2,8]	→[3,8]	→[4,8]	→[5,8]	→[6,8]	→[7,8]	#19	#20	#21	#22	→[8,9]	→[8,8]
g_9	A si B	→[1,9]	→[2,9]	→[3,9]	→[4,9]	→[5,9]	→[6,9]	→[7,9]	→[8,9]	→[8,8]	→[8,10]	→[8,10]	→[8,13]	→[8,12]
g_{10}	A d B	→[1,10]	→[2,10]	→[3,10]	→[4,10]	→[5,10]	→[6,10]	→[7,10]	→[8,10]	→[9,10]	#23	#24	→[10,9]	→[10,8]
g_{11}	A di B	→[1,11]	→[2,11]	→[3,11]	→[4,11]	→[5,11]	→[6,11]	→[7,11]	→[8,11]	→[9,11]	→[10,11]	→[10,11]	→[10,13]	→[10,12]
g_{12}	A f B	→[1,12]	→[2,12]	→[3,12]	→[4,12]	→[5,12]	→[6,12]	→[7,12]	→[8,12]	→[9,12]	→[10,12]	→[11,12]	→[11,12]	→[8,8]
g_{13}	A fi B	→[1,13]	→[2,13]	→[3,13]	→[4,13]	→[5,13]	→[6,13]	→[7,13]	→[8,13]	→[9,13]	→[10,13]	→[11,13]	→[12,13]	→[12,12]

primitive case

axes ordering
symmetry

2D operands
ordering symmetry

synchronized axes
flipping symmetry

asynchronized y-axis
flipping symmetry

Figure 4: The 13×13 cases of 2D Allen's interval algebra. It shows 24 primitive cases for scatter plots as numbered in Figure 3, and a transformation path from each of other cases to one of the primitive cases.

transformations can be expressed as follows:

$$\begin{aligned}
 & \Psi_{AXFS}([g_i(A_x, B_x), g_s(A_y, B_y)]) \\
 & \rightarrow [\Psi_{AFS}(g_i(A_x, B_x)), g_s(A_y, B_y)] \\
 & \rightarrow [g_j(A_x^-, B_x^-), g_s(A_y, B_y)]
 \end{aligned} \quad (6)$$

$$\begin{aligned}
 & \Psi_{AYFS}([g_i(A_x, B_x), g_s(A_y, B_y)]) \\
 & \rightarrow [g_i(A_x, B_x), \Psi_{AFS}(g_s(A_y, B_y))] \\
 & \rightarrow [g_j(A_x, B_x), g_t(A_y^-, B_y^-)]
 \end{aligned} \quad (7)$$

When one of the 169 cases can be transformed to another

using any above transformation, they are said to be *topologically isomorphic*. Since it is relatively trivial to prove that all above-mentioned transformations are communicative, such a isomorphism is *symmetric*. When a number of cases form an *isomorphic group*, where each case can be transformed to another through one or more transformations. For each isomorphic group, we can select one case as the primitive case. Figure 3 shows 24 primitive cases of Allen's interval algebra in 2D for scatter plots. Figure 4 illustrates some of the symmetric transformations that lead to the formation of these 24 isomorphic groups. Figure 5 shows 35 primitives

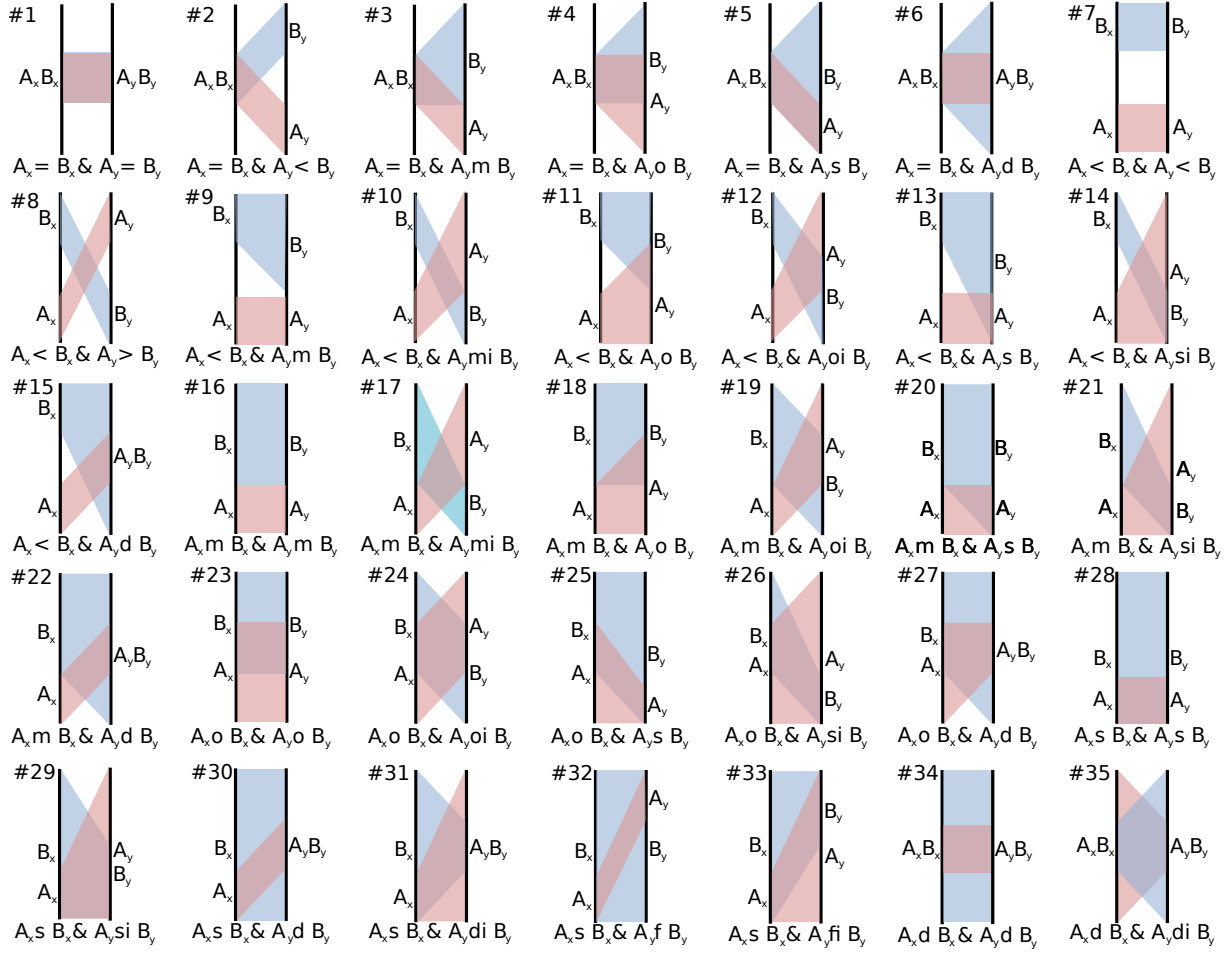


Figure 5: 169 parallel coordinates cases can be reduced to a subset of 35 topologically distinct base cases using 4 symmetries.

cases for parallel coordinates, while Figure 6 illustrates the formation of the isomorphic groups.

4.2. Computational Verification of the Primitive Cases

We established the isomorphic groups using two different methods. Firstly we used the matrices in Figure 3 and Figure 4 as exhaustive lists of all cases in the two types of plots respective. We sketched out many cases to identify symmetric transformation from one another. Secondly, we enumerated all possible symmetric transformations computationally, providing a verification of the isomorphic groups found manually. The algorithm for forming each isomorphic group by searching for all possible symmetric transformations is described below. The algorithm demonstrates the establishment of isomorphic groups in 1D. Consider the list of 13 cases, each with an operator g_i , as in Figure 1. Procedure 1 exhaustively visits each non-isomorphic case, and applies the rules in the rule set, $\{\Psi_{OOS}, \Psi_{AFS}, \Psi_{OOS} \circ \Psi_{AFS}\}$ based on Equations 1 and 2, where \circ denotes the applications of


Procedure 1 Exhaustive isomorphic elimination in 1D.

```


1: procedure VERIFY1D
2:    $F[1..13] \leftarrow 0$            ▷ initialize all non-isomorphic
3:   for each  $g_i \in$  Operator Set do
4:     if  $F[i] = 0$  then
5:       for each rule  $\Psi \in$  Rule Set do
6:          $[h, U, V] \leftarrow \Psi(g_i, A_i, B_i)$            ▷ transform
7:         for each  $k \in [1..13] \wedge k \neq i$  do
8:           if  $F[k] = 0 \wedge EQ([h, U, V], [g_k, A_k, B_k])$  then
9:              $F[k] \leftarrow i$            ▷ set isomorphic link
10:          end if
11:        end for
12:      end for
13:    end if
14:  end for
15: end procedure

```


		y												
x		g_1	g_2	g_3	g_4	g_5	g_6	g_7	g_8	g_9	g_{10}	g_{11}	g_{12}	g_{13}
		A = B	A < B	A > B	A m B	A mi B	A o B	A oi B	A s B	A si B	A d B	A di B	A f B	A fi B
g_1	A = B	#1	#2	→[1,2]	#3	→[1,4]	#4	→[1,6]	#5	→[1,8]	#6	→[1,10]	→[1,8]	→[1,12]
g_2	A < B	→[1,2]	#7	#8	#9	#10	#11	#12	#13	#14	#15	→[3,10]	→[3,9]	→[3,8]
g_3	A > B	→[1,3]	→[2,3]	→[2,2]	→[2,5]	→[2,4]	→[2,7]	→[2,6]	→[2,9]	→[2,8]	→[2,10]	→[2,10]	→[2,13]	→[2,12]
g_4	A m B	→[1,4]	→[2,4]	→[3,4]	#16	#17	#18	#19	#20	#21	#22	→[5,10]	→[5,9]	→[5,8]
g_5	A mi B	→[1,5]	→[2,5]	→[3,5]	→[4,5]	→[4,4]	→[4,7]	→[4,6]	→[4,9]	→[4,8]	→[4,10]	→[4,10]	→[4,13]	→[4,12]
g_6	A o B	→[1,6]	→[2,6]	→[3,6]	→[4,6]	→[5,6]	#23	#24	#25	#26	#27	→[7,10]	→[7,9]	→[7,8]
g_7	A oi B	→[1,7]	→[2,7]	→[3,7]	→[4,7]	→[5,7]	→[6,7]	→[6,6]	→[6,9]	→[6,8]	→[6,10]	→[6,10]	→[6,13]	→[6,12]
g_8	A s B	→[1,8]	→[2,8]	→[3,8]	→[4,8]	→[5,8]	→[6,8]	→[7,8]	#28	#29	#30	#31	#32	#33
g_9	A si B	→[1,9]	→[2,9]	→[3,9]	→[4,9]	→[5,9]	→[6,9]	→[7,9]	→[8,9]	→[8,8]	→[8,10]	→[8,10]	→[8,13]	→[8,12]
g_{10}	A d B	→[1,10]	→[2,10]	→[3,10]	→[4,10]	→[5,10]	→[6,10]	→[7,10]	→[8,10]	→[9,10]	#34	#35	→[10,9]	→[10,8]
g_{11}	A di B	→[1,11]	→[2,11]	→[3,11]	→[4,11]	→[5,11]	→[6,11]	→[7,11]	→[8,11]	→[9,11]	→[10,11]	→[10,10]	→[10,13]	→[10,12]
g_{12}	A f B	→[1,12]	→[2,12]	→[3,12]	→[4,12]	→[5,12]	→[6,12]	→[7,12]	→[8,12]	→[9,12]	→[10,12]	→[11,12]	→[8,8]	→[8,9]
g_{13}	A fi B	→[1,13]	→[2,13]	→[3,13]	→[4,13]	→[5,13]	→[6,13]	→[7,13]	→[8,13]	→[9,13]	→[10,13]	→[11,13]	→[12,13]	→[12,12]




primitive case



axes ordering symmetry



2D operands ordering symmetry



synchronized axes flipping symmetry

Figure 6: The 13×13 cases of 2D Allen’s interval algebra. It shows 35 primitive cases for parallel coordinates plots as numbered in Figure 5, and a transformation path from each of other cases to one of the primitive cases.

two rules (right first). If the application of a rule to $g_i(A_i, B_i)$ resulting in $h(U, V)$ that is topologically equitant to another case g_k , then g_k is an isomorphic with g_i and g_k is eliminated for further consideration.

Procedure 2 shows an algorithm that exhaustively searches isomorphic group in 2D for scatter plots and parallel coordinates. The rule set for parallel coordinates are based on Equations 3, 4 and 5, resulting in $\{\Psi_{2d-OOS}, \Psi_{SAFS}, \Psi_{AOS}, \Psi_{2d-OOS} \circ \Psi_{SAFS}, \Psi_{2d-OOS} \circ \Psi_{AOS}, \Psi_{SAFS} \circ \Psi_{AOS}, \Psi_{2d-OOS} \circ \Psi_{SAFS} \circ \Psi_{AOS}\}$. These rules are also used for scatter plots. However to achieve full reduction, further rules are required based on Equations 6 and 7, including $\{\Psi_{AXAFS}, \Psi_{AYAFS}, \Psi_{2d-OOS} \circ \Psi_{AXAFS}, \Psi_{2d-OOS} \circ \Psi_{AYAFS}, \Psi_{AXAFS} \circ \Psi_{AOS}, \Psi_{AYAFS} \circ \Psi_{AOS}, \Psi_{2d-OOS} \circ \Psi_{AXAFS} \circ \Psi_{AOS}, \Psi_{2d-OOS} \circ \Psi_{AYAFS} \circ \Psi_{AOS}\}$. The rule set does not contain all combinations of the rules because commutative laws apply. In addition, we have $\Psi_{SAFS} \circ \Psi_{AXAFS} = \Psi_{AYAFS}$ and so on. Running Procedure 2 confirmed 24 primitive cases for scatter plots in Figure 3 and 35 primitive cases for parallel coordinates in Figure 5.

5. Estimating Visual Complexity

Given a relatively small number of primitive cases in either cluster-based scatter plot or parallel coordinates, we can consider the notion of *visual complexity* in a relatively abstract manner by focusing on topological differences between these cases. In this section, we first propose a scheme for estimating a *complexity score* for each primitive case. We then compare the scores with a collection of samples that

Procedure 2 Exhaustive isomorphic elimination in 2D.

```

1: procedure VERIFY2D
2:    $F[1..13][1..13] \leftarrow 0$   $\triangleright$  initialize all non-isomorphic
3:   for each  $g_i \in$  Operator Set do
4:     for each  $g_s \in$  Operator Set do
5:       if  $F[i][s] = 0$  then
6:         for each rule  $\Psi \in$  Rule Set do
7:            $H \leftarrow [h_x, U_x, V_x; h_y, U_y, V_y]$ 
8:            $G \leftarrow [g_{i,x}, A_{i,x}, B_{i,x}; g_{s,y}, A_{i,y}, B_{i,y}]$ 
9:            $H \leftarrow \Psi(G)$   $\triangleright$  transform
10:          for each  $k, l \in [1..13][1..13] \wedge k, l \neq i, s$  do
11:            if  $F[k][l] = 0 \wedge EQ(H, G)$  then
12:               $F[k][l] \leftarrow \langle i, s \rangle$  set isomorphic link
13:            end if
14:          end for
15:        end for
16:      end if
17:    end for
18:  end procedure

```

record how human observers may perceive visual complexity. Finally, we provide a means for approximating n -cluster visual complexity.

5.1. Estimating 2-cluster Complexity

The purpose of estimating visual complexity is to provide a metric for measuring some aspects of visual uncertainty as discussed in [DCK12]. Allen’s interval algebra takes into

account both overlapping and “meeting” clusters as topological features. Hence an estimation scheme must encode both features, and it may have the following principal considerations:

1. A primitive case should receive the lowest complexity score if it consists of two clusters that neither overlap nor meet with each other. We make 0 the lowest complexity score.
2. A primitive case should receive the highest complexity score if it consists two clusters that are equal on both axes, i.e., totally coinciding with one another. We make 1 the highest complexity score.
3. When shape A is not overlapped by shape B , A is visually less complex than when it is crossed over by shape B .
4. When shape A has at least one non-overlapping region, A is visually less complex than when it is totally overlapped by B .
5. When shape A is split by shape B into three pieces (1 overlapping and 2 non-overlapping), A is visually more complex than when A is split by B into two pieces (1 overlapping and 1 non-overlapping).
6. When A and B meet at $k + 1$ corners, the case is visually more complex than when they meet at k corners ($k > 0$).
7. When A and B meet only at a corner, the case is visually less complex than when they meet along an edge.

Scoring the 24 Primitive Cases of Scatter Plots. Given two rectangular shapes A and B representing two clusters in a scatter plot, we consider an estimation scheme that decomposes a complexity score U into four components as $U = U_A + U_B + U_{AB} + U_m$.

- $U_A = 0.0$ if shape A has one continuous non-overlapping region. $U_A = 0.1$ if A has two disconnected non-overlapping regions. $U_A = 0.2$ if A has no non-overlapping region at all.
- U_B is scored in the same way as U_A by exchanging the relationship between A and B .
- $U_{AB} = 0.0$ if A and B do not overlap, and $U_{AB} = 0.2$ otherwise (i.e., there is one overlapping region).
- $U_m = 0.1 \times n_e$ where n_e is the number of edges where A and B meet. $U_m = 0.1$ if A and B do not meet at any edge but at a corner point.

Figure 7 show some examples that illustrate the scores of U_A , U_B , U_{AB} and U_m individually. Figure 9 lists the scores of U for all 24 primitive cases of scatter plots. Note that when A and B coincide completely, U sums up to exactly 1.

Scoring the 35 Primitive Cases of Parallel Coordinates. Given two quadrilateral or triangular shapes A and B representing two clusters in a parallel plot, we consider a similar estimation scheme that decomposes a complexity score into four components. The first three components U_A , U_B and U_{AB} are computed in the same way as with scatter plots. U_m is computed is a slightly different way.

- $U_m = 0.1 \times n_p$ where n_p is the number of corner points where A and B meet.

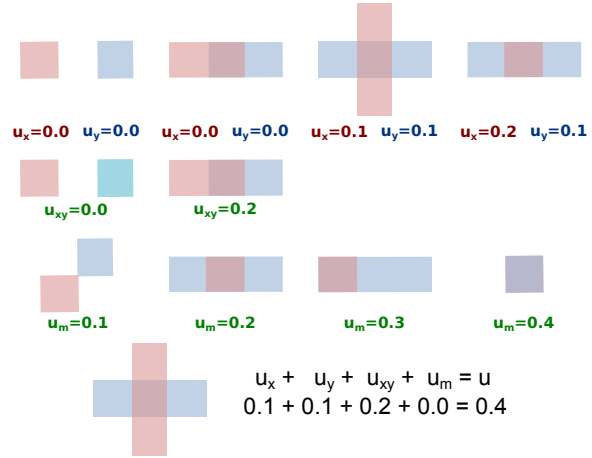


Figure 7: Uncertainty approximation for scatter plots.

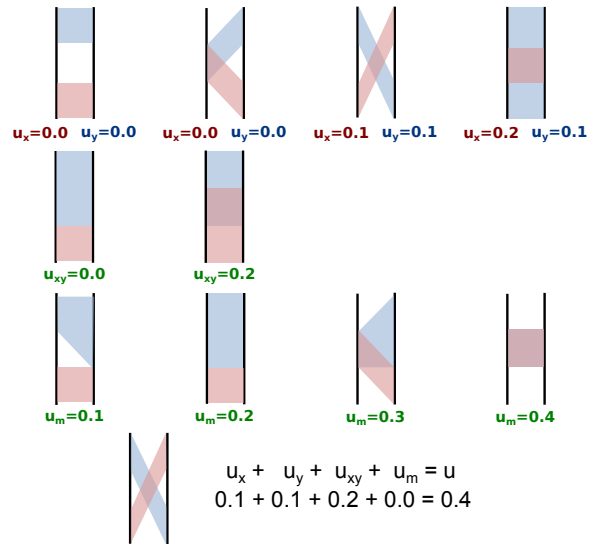


Figure 8: Uncertainty approximation for parallel coordinates.

Figure 8 show some examples that illustrate the scores of U_A , U_B , U_{AB} and U_m individually. Figure 9 lists the scores of U for all 35 primitive cases of parallel plots.

5.2. Comparison with Human Estimation

We consulted 29 volunteers, including 11 visualization researchers and 18 with statistics, mathematics, humanities and non-academic backgrounds. We asked them how they would make a comparative judgement about visual complexity. Through a web-based interface, participants compared pairs of randomly generated primitive cases. For each pair placed side-by-side, the participants were asked make a choice among three options: “Left is less complex than

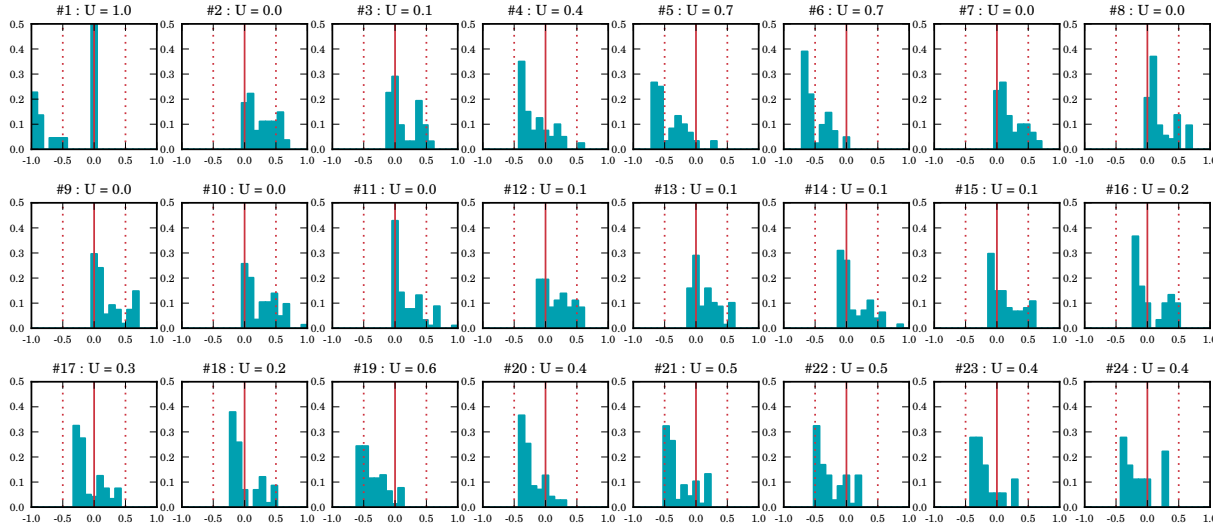


Figure 9: Scatter plot case distributions show the amount of agreement of measured perceived visual complexity with our scoring system. The scatter score is in the title of each plot.

Right”, “*Left is more complex than Right*”, or “*Left and Right have similar complexity*”. Participants compared 50 scatter plot pairs and 50 parallel coordinate pairs in two trial.

We purposely did not introduce the term *uncertainty* to the participants as the interpretation of each primitive case can be made uncertain for the given information as long as there is sufficient time. Instead, we simply consult the participants about which “case is more visually confusing than another”. We left the participants to make their own judgement of the definition of term *confusing*, hence the meaning of *visual complexity*.

The majority of participants used their intuition to compare pairs of patterns. Figure 9 shows 24 bar charts for each scatter plot case and Figure 10 shows 35 bar charts for each parallel coordinate case. In each bar chart, the $k = 0$ -bar indicates the number of times when the observer made the same judgement as the estimation scheme in Section 5.1 when comparing this specific case A against a case X randomly selected from the 35 primitive cases. The $+k$ bars indicate when the observer over estimated the complexity for our scoring of a case, while $-k$ bars indicate the observers under estimate of the complexity. The estimation scheme scores A k points higher than X . We consider a $[-0.1, +0.1]$ error in judgement an acceptable threshold for determining consistency of human observed measures for our scoring system.

The judgements by different human observers are not consistent. We observe for the scatter plots from Figure 9 that for most cases the distribution is clustered around the 0-bar with an error of approximately $[-0.5, +0.5]$. This is surprising, as scatter plots are generally considered to be a simpler data representation than parallel coordinates. The distributions are spread broadly with a few cases showing noticeable

over estimates, (cases 2, 7, 9, 10) or under estimates (cases 5, 6, 19). This suggests that although topologically, scatter-plots are the simpler representation, observers have difficulty in judging the relationships between clusters on orthogonal axes. In contrast, Figure 10 shows tighter clusters more consistent with the parallel coordinates complexity scoring. There are more obvious overestimating cases (7, 9, 11, 16, 23), and a few underestimating cases (5, 30, 32). Overall human estimations are less dispersed with the parallel coordinates possibly because the topology is more constrained as clusters are limited in where they appear on parallel axes.

We examined these cases in detail. Some inconsistency can be explained. For example, the underestimation in case 1 for both plots is largely because the participants mistook the two totally overlapped shapes as a single shape. This actually confirms that the computer score of 1 is correct. We also made attempts to alter the estimation scheme. However, we could not find a better scheme, as each attempted change only resulted in more over- or under-scores in other cases. We believe that this is an interesting research problem for future work. One possibility is to conduct a large scale collection of the judgements of human observers. From such empirical data, one may be able to establish a better estimation scheme, or simply make the mean values of the human observations as the scores. Such an empirical study is beyond the scope of this work.

5.3. Approximating n -cluster Complexity

In practice, both scatter plots and parallel coordinates are expected to handle more than 2 clusters. The extension of Allen’s interval algebra from a 2-operand algebra to an n -operand algebra is a non-trivial challenges. We hence

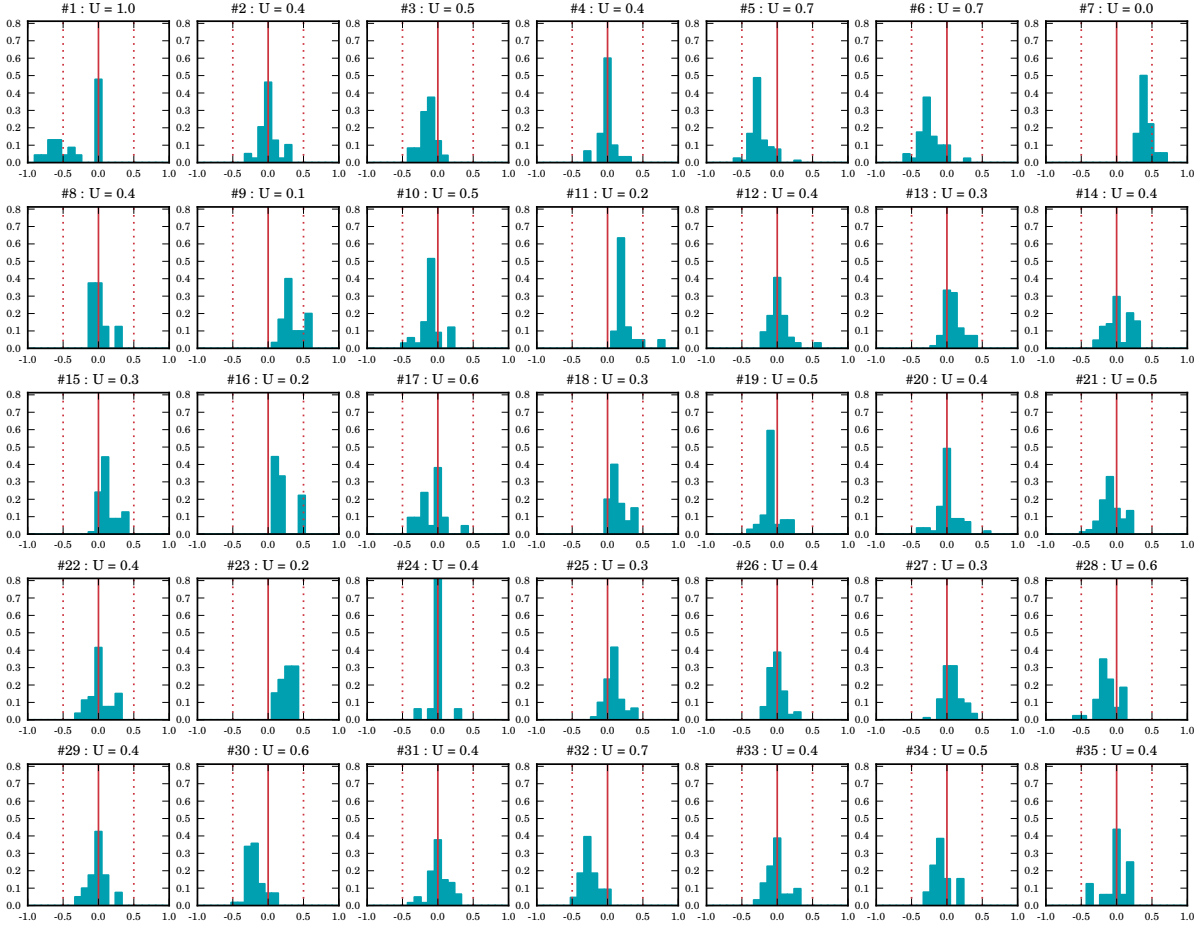


Figure 10: Parallel coordinates case distributions show the amount of agreement of measured perceived visual complexity with our scoring system. The parallel score is in the title of each plot.

address this need by approximating n -cluster complexity by making use of the 2-cluster estimation scheme. Let A_1, A_2, \dots, A_n be n clusters. Let $\sigma_2(A_i, A_j)$ be a 2-cluster score of the pair A_i vs. A_j , where $i, j = 1, 2, \dots, n$. We can approximate the n -cluster score σ_n as:

$$\sigma_n(A_1, A_2, \dots, A_n) = \frac{2}{n(n-1)} \sum_{i=1}^{n-1} \sum_{j=i+1}^n \sigma_2(A_i, A_j)$$

The average is also a quantity in $[0.0, 1.0]$ as $\sigma_2(A_i, A_j)$.

6. Conclusions & Future Work

This is a theoretical study on visual complexity in the context of cluster visualization. The central thesis is that it is possible to use Allen's interval algebra to derive a scheme for estimating visual complexity. As this is an ambitious thesis, this work is merely the first step to bring mathematics and user experience together. We have confirmed, both manually

and computationally, the primitive cases in 2D Allen's interval algebra, which is useful for reducing the look-up cases for the estimation scheme. We have formulated estimation schemes for scatter plots and parallel coordinates plots. We have collected some human estimations about visual complexity in relation to these two plots. In comparison with the subjective judgements by humans, our estimation schemes are promising.

This research points to a number of interesting and challenging directions for future studies. These include the need for us to gain further understanding about how humans estimate visual complexity (e.g., how geometry and topology interfere with each other). As the sampling space is fairly large (e.g., 35×35 for parallel coordinates plots), this would require a large scale empirical study with carefully designed stimuli. We hope to continue this work, and use both mathematics and empirical studies to create quantitative metrics for visualization.

References

- [AA04] ANDRIENKO G., ANDRIENKO N.: Parallel coordinates for exploring properties of subsets. In *Proc. Coordinated and Multiple Views in Exploratory Visualization* (2004), IEEE, pp. 93–104. [1](#)
- [AdOL04] ARTERO A. O., DE OLIVEIRA M. C. F., LEVKOWITZ H.: Uncovering clusters in crowded parallel coordinates visualizations. In *Proc. IEEE Information Visualization* (2004), IEEE, pp. 81–88. [2](#)
- [All83] ALLEN J. F.: Maintaining knowledge about temporal intervals. *Communications of the ACM* (November 1983), 832–843. [2](#)
- [BS06] BERTINI E., SANTUCCI G.: Visual quality metrics. In *Proc. BELIV Workshop* (2006), pp. 1–5. [2](#)
- [CDD06] CARR H., DUFFY B., DENBY B.: On histograms and isosurface statistics. *IEEE Transactions on Visualization and Computer Graphics* 12, 5 (2006), 1259–1266. [2](#)
- [DCK12] DASGUPTA A., CHEN M., KOSARA R.: Conceptualizing visual uncertainty in parallel coordinates. *Computer Graphics Forum* 31, 3pt2 (june 2012), 1015–1024. [1](#), [6](#)
- [DCT12] DUFFY B., CARR H., TORSTEN M.: Integrating isosurface statistics and histograms. *IEEE Transactions on Visualization and Computer Graphics* 14 (2012). [2](#)
- [DK10] DASGUPTA A., KOSARA R.: Pargnostics: Screen-space metrics for parallel coordinates. *IEEE Transactions on Visualization and Computer Graphics* 16, 6 (2010), 1017–26. [2](#), [3](#)
- [DK11] DASGUPTA A., KOSARA R.: Adaptive privacy-preservation using parallel coordinates. *IEEE Transactions on Visualization and Computer Graphics* 17, 12 (2011), 2241–2248. [2](#)
- [ED06] ELLIS G., DIX A.: Enabling automatic clutter reduction in parallel coordinate plots. *IEEE Transactions on Visualization and Computer Graphics* 12, 5 (2006), 717–724. [2](#)
- [ED07] ELLIS G., DIX A.: A taxonomy of clutter reduction for information visualisation. *IEEE Transactions on Visualization and Computer Graphics*, 13, 6 (2007), 1216–1223. [2](#)
- [FWR99] FUA Y.-H., WARD M. O., RUNDENSTEINER E. A.: Hierarchical parallel coordinates for exploration of large datasets. In *Proc. IEEE Visualization* (1999), IEEE CS Press, pp. 43–50. [1](#)
- [HMS09] HARPER S., MICHAILIDOU E., STEVENS R.: Toward a definition of visual complexity as an implicit measure of cognitive load. *ACM Transactions on Applied Perception* 6, 2 (2009), 10:1–10:18. [1](#)
- [ID90] INSELBERG A., DIMSDALE B.: Parallel coordinates: A tool for visualizing multi-dimensional geometry. In *Proc. IEEE Visualization* (1990), IEEE CS Press, pp. 361–378. [1](#)
- [JLJC05] JOHANSSON J., LJUNG P., JERN M., COOPER M.: Revealing structure within clustered parallel coordinates displays. In *Proc. IEEE Symposium on Information Visualization* (2005), pp. 125–132. [2](#)
- [KW10] KHOURY M., WENGER R.: On the fractal dimension of isosurfaces. *IEEE Transactions on Visualization and Computer Graphics* 16, 6 (Nov.-Dec. 2010), 1198–1205. [2](#)
- [LC87] LORENSEN W. E., CLINE H. E.: Marching cubes: a high resolution 3D surface construction algorithm. In *Proc. ACM SIGGRAPH* (New York, NY, USA, 1987), pp. 163–169. [1](#)
- [NH06] NOVOTNY M., HAUSER H.: Outlier-preserving focus+context visualization in parallel coordinates. *IEEE Transactions on Visualization and Computer Graphics* 12, 5 (2006), 893–900. [1](#)
- [PWR04] PENG W., WARD M., RUNDENSTEINER E.: Clutter reduction in multi-dimensional data visualization using dimension reordering. In *Proc. IEEE Information Visualization* (2004), IEEE CS Press, pp. 89–96. [2](#)
- [RLN07] ROSENHOLTZ R., LI Y., NAKANO L.: Measuring visual clutter. *Journal of Vision* 7, 2 (2007). [2](#)
- [SBSÇ10] SCHNUR S., BEKTAŞ K., SALAHİ M., ÇÖLTEKİN A.: A comparison of measured and perceived visual complexity for dynamic web maps. In *Proc. 6th International Conference on Geographic Information Science* (2010). [1](#)
- [SSD*08] SCHEIDEGGER C. E., SCHREINER J. M., DUFFY B., CARR H., SILVA C. T.: Revisiting histograms and isosurface statistics. *IEEE Transactions on Visualization and Computer Graphics* 14, 6 (2008), 1659–1666. [2](#)
- [ZYQ*08] ZHOU H., YUAN X., QU H., CUI W., CHEN B.: Visual clustering in parallel coordinates. *Computer Graphics Forum* 27, 3 (2008), 1047–1054. [2](#)